

## A COMPRESSIBLE CFD METHOD FOR FLOW WITH SOUND FROM VERY LOW MACH NUMBER TO SUPERSONIC

Eiji Shima\*

\* Japan Aerospace Exploration Agency  
3-1-1, Yoshinodai, Sagamihara, Kanagawa, 229-8510, Japan  
e-mail:shima.eiji@jaxa.jp

**Keywords:** AUSM, SHUS, LSHUS, Riemann flux

**Abstract.** *In some aerodynamic application, both of compressible and incompressible fluid phenomena have importance. Aero-acoustic sound generated by bluff bodies in low Mach number flows is one of this kinds of applications. The compressible flow CFD method can potentially solve flow and sound in the same framework. We present new compressible CFD method that can compute the flow with sound propagation from very low Mach number. This method is based on MUSCL approach of the third order spatial accuracy with a new Riemann flux function of AUSM family name LSHUS. The key idea is to control the numerical viscosity in low Mach number regime. The resulting new scheme inherits the advantage that ASUM family scheme have, for examples, robustness, accuracy and simplicity while reducing the numerical diffusion in low Mach number. In addition it can compute sound propagation and vortices with less dissipation than existing schemes. The formulation of the scheme is led and then some numerical example are shown, such as, sound propagation, vortex, flow around cylinder at various Mach number.*

## 1 INTRODUCTION

In some aerodynamic applications, both of the compressible and incompressible effects are important. Aero-acoustic sound generated by bluff bodies in low Mach number flows is one of this kind of applications. Since the incompressible flow CFD method cannot compute sound propagation directly, it must be computed separately from flow computation. It is necessary to use FEM or similar method to compute sound propagation in a complex field and it needs similar computational costs to solve inviscid compressible flow equation when the unsteady computation is required.

On the other hand, the compressible flow CFD method can potentially solve flow and sound in one framework. In order to compute very low Mach number flows, it is known that the preconditioning matrix<sup>[1-3]</sup> method is very effective. This matrix works at two phases in the flow solver. One is the time integral preconditioning and the other is numerical dissipation preconditioning. The former dramatically improve the convergence to the steady states in low Mach number flows. However, it cannot directly treat sound propagation. This is because the preconditioning matrix completely changes sound speed. The latter only controls the numerical dissipation of the scheme within the proper amount in low Mach number flow. Thus it can compute the sound propagation. The preconditioned methods in the latter sense, however, have several defects. Firstly, most of them contain problem dependent parameters. The smaller the parameters are, the less the numerical dissipation becomes. However, the parameters must not be zero in order for stable computations. Therefore user must trade quality between stability. Secondly, the preconditioning methods tends to work as the original unpreconditioned scheme beyond transonic speed regime, thus they have the weak points that the original schemes have, for example the lack of robustness of Roe's flux difference splitting scheme<sup>[4]</sup> in supersonic speed, although Roe scheme is widely recognized as one of the most well known approximate Riemann flux functions. Therefore we have to think about the choice of the Riemann flux functions, since it have much influence on stability, accuracy and efficiency of the method. The Riemann flux function originally gives flux at interface of two different fluid states by exactly solving the Riemann initial value problem. However, it takes much cost to compute exactly and the approximate value is enough for numerical computations. In addition, Riemann solution itself is not needed. Therefore approximate schemes are used more widely, and we call a function as a Riemann flux functions if it gives proper value at the interface. Roe's approximate Riemann flux functions is one of the early developed function of this kind, and have been widely used as basis of compressible CFD algorithm for its relative simplicity, theoretical clearness and accuracy for solving discontinuity such as shock or contact surface. The defects of Roe scheme stated above are widely known too.

In order to overcome such problems, a number of schemes have been proposed. Among them, AUSM (Advection Upstream Splitting Method), originally developed by Liou and Steffen<sup>[5]</sup>, and its variant AUSM-family schemes<sup>[6-8]</sup> are simple, yet accurate and robust for high Mach number flows. Thus they have been widely used as the standard methods of compressible CFD algorithms.

In recent years, there are researches to incorporate the preconditioning matrix method to AUSM-family scheme in order to formulate the all-speed scheme that can compute the flow from very low Mach number to very high Mach number by the same scheme<sup>[9,10]</sup>. However, these schemes lose simplicity in their formulations that the original AUSM has. In addition, these methods lack universal applicability for the practical use, since they need problem-dependent parameters specified by the user.

The purpose of this study is to develop an all-speed scheme of AUSM-family in a simpler form without tunable parameters. Firstly, the AUSM-family schemes are briefly described,

and then, the new simple mass flux function and pressure function are introduced, which reduce numerical dissipation in low Mach number regime. Then, a new scheme named LSHUS (Low-dissipation Simple High-resolution Upwind Scheme) is presented. The relationship between the preconditioning methods is also shown. Finally, by comparing with existing methods, its advantages are demonstrated in the flow computations involving fundamental flow features, such as a shock, a vortex, a boundary-layer separation, and sound propagations, in wide-ranging Mach number regime. The simple implicit time integration method which is used in this study is also shown in APPENDIX.

## 2 NUMERICAL SCHEME

### 2.1 Cell centered finite volume method and MUSCL approach

The governing equation is Navies-Stokes equation. It is discretized using the general (structured or unstructured) cell centered finite volume method written as follows,

$$\frac{V_i}{\Delta t_i} \Delta \mathbf{Q}_i + \sum_j (\tilde{\mathbf{E}}_{i,j} - \tilde{\mathbf{R}}_{i,j}) s_{i,j} = 0 \quad (1)$$

$$\mathbf{Q} = (\rho, \rho u, \rho v, \rho w, e)^T \quad (2)$$

$$\Delta \mathbf{Q}_i = \mathbf{Q}_i^{n+1} - \mathbf{Q}_i^n \quad (3)$$

where  $\mathbf{Q}$  is a vector of the conservative variables,  $\tilde{\mathbf{E}}_{i,j}$  and  $\tilde{\mathbf{R}}_{i,j}$  are inviscid and viscous flux vector through the surface of a control volume (computational cell),  $s_{i,j}$  is the area of cell interface,  $V_i$  is the volume of the cell,  $\rho, u, v, w, e$  are density, components of velocity, total energy, respectively. Conservative variables are defined at the center of the computational cell, and whole difference of the numerical scheme in this formulation comes from the definition of fluxes at cell interface.

Since inviscid terms have crucial importance for high Reynolds number flow, only Euler equation is presented for the numerical scheme. Viscous fluxes are computed using second order central difference formula in this study. The inviscid flux can be written as;

$$\tilde{\mathbf{E}} = \dot{m} \mathbf{\Phi} + p \mathbf{N} \quad (4)$$

$$\mathbf{\Phi} = (1, u, v, w, h)^T, \quad (5)$$

$$\mathbf{N} = (0, x_n, y_n, z_n, 0)^T \quad (6)$$

$$\dot{m} = \rho(x_n u + y_n v + z_n w) = \rho V_n, \quad (7)$$

$$h = \frac{e + p}{\rho}, \quad (8)$$

$$p = (\gamma - 1) \left( e - \frac{\rho}{2} (u^2 + v^2 + w^2) \right), \quad (9)$$

where  $p, \gamma, \dot{m}, x_n, y_n, z_n$  are pressure, specific heat ratio, mass flux, and normal vector of cell face respectively.

The equation is discretized by cell centered finite volume method stated above using the third order MUSCL. In this approach, distributions of primitive variables are reconstructed in each cell and then fluxes are computed by the Riemann flux. For example, this procedure can be written in one dimension as;

$$\mathbf{U}_{i+1/2}^+ = \mathbf{U}_i + \frac{1}{4}(1 + \kappa)(\mathbf{U}_{i+1} - \mathbf{U}_i) + \frac{1}{4}(1 - \kappa)(\mathbf{U}_i - \mathbf{U}_{i-1}), \quad (10)$$

$$\mathbf{U}_{i+1/2}^- = \mathbf{U}_{i+1} - \frac{1}{4}(1 + \kappa)(\mathbf{U}_{i+2} - \mathbf{U}_{i+1}) - \frac{1}{4}(1 - \kappa)(\mathbf{U}_{i+1} - \mathbf{U}_i), \quad (11)$$

$$\tilde{\mathbf{F}} = \tilde{\mathbf{F}}(\mathbf{U}_{i+1/2}^+, \mathbf{U}_{i+1/2}^-), \quad (12)$$

where  $\mathbf{U}, \tilde{\mathbf{F}}$  are vectors of primitive variables and Riemann flux function, and  $\kappa=1/3$  is used, with which the third order accuracy is obtained in one dimensional case. Note that superscripts + and - denote left and right side of the cell interface where the normal vector points from left to right. AUSM-family schemes are adopted in this study as the Riemann flux function. The Riemann flux function of AUSM-family schemes can be written as,;

$$\tilde{\mathbf{F}} = \frac{\dot{m} + |\dot{m}|}{2} \mathbf{\Phi}^+ + \frac{\dot{m} - |\dot{m}|}{2} \mathbf{\Phi}^- + \tilde{p}\mathbf{N} \quad (13)$$

Note that the mass flux  $\dot{m}$  and the averaged pressure  $\tilde{p}$  are given by proper numerical algorithms. The different definitions of them produce different kind of AUSM family schemes.

## 2.2 Selection of mass flux

The mass flux of original AUSM is shown below;

$$\dot{m}_{AUSM} = \frac{\hat{M} + |\hat{M}|}{2} \rho^+ c^+ + \frac{\hat{M} - |\hat{M}|}{2} \rho^- c^-, \quad (14)$$

$$\hat{M} = \tilde{M}^+ + \tilde{M}^-, \quad (15)$$

$$\tilde{M}^\pm = \begin{cases} \pm \frac{1}{4}(M^\pm \pm 1)^2, & \text{if } |M^\pm| < 1 \\ \frac{M_\pm \pm |M_\pm|}{2}, & \text{otherwise} \end{cases}, \quad (16)$$

where  $M$  denotes Mach number normal to the cell face. The authors proposed<sup>[8]</sup> SHUS (Simple High-resolution Upwind Scheme) in which mass flux of the original AUSM was replaced by that of Roe scheme, and showed that SHUS cured spurious overshoots appeared at a shock front in the case of the original AUSM. The mass flux of SHUS is written as follows.

$$\begin{aligned}
\dot{m}_{SHUS} = & \frac{1}{2} \left\{ (\rho V_n)^+ + (\rho V_n)^- \right. \\
& - |\bar{V}_n| \Delta \rho \\
& - \frac{|\bar{M} + 1| - |\bar{M} - 1|}{2} \bar{\rho} \Delta V_n \\
& \left. - \frac{|\bar{M} + 1| + |\bar{M} - 1| - 2|\bar{M}|}{2\bar{c}} \Delta p \right\} \\
\Delta q = & q^- - q^+
\end{aligned} \tag{17}$$

where  $(\bar{\quad})$  stands for arithmetic averages of both sides (this holds also in the rest of the paper). The formulation of SHUS might look more complex than that of AUSM, however, computational cost indeed slightly less since no “if” statement is contained in the coding.

AUSM<sup>+[5]</sup>, that is revised version of AUSM, overcomes the overshoot for the grid aligned shock, however, there still remains problem for the non-grid aligned one. On the other hand SHUS has no such problems. The noticeable difference between SHUS and AUSM/AUSM<sup>+</sup> in their formulation is the term of pressure difference in mass flux shown at 4<sup>th</sup> term in the right-hand side of Eq.(17). As pointed out by Liou<sup>[11]</sup>, this term tends to cause the carbuncle phenomena in some hypersonic flows. However, SHUS is still more stable than Roe scheme. Note that such phenomena only appear at strong shock wave, thus the care is not needed for the flows under transonic speed. It is reported in the recent literatures that similar pressure difference term included in mass flux augments stability at very low Mach number. For example, schemes shown in Ref.[7] and Ref.[12] contain that term with adjustable coefficients. On the other hand the term in SHUS is derived from correct upwind mass flux for linearized Euler equation, i.e. from Roe scheme. Therefore this term is more rigorously derived. Thus the mass flux of SHUS is adopted in this study.

### 2.3 Controlling numerical viscosity at low Mach number

Since a Riemann flux function is essentially a first order upwind scheme, it contains numerical viscosity proportional to local characteristic speed. However, this fact is not apparent from the formulation of AUSM family schemes. We will show they also have that common nature in their pressure term inheriting from van Leer’s flux vector splitting scheme<sup>[13]</sup>. The pressure term of AUSM-family scheme is written as,

$$\tilde{p} = \beta^+ p^+ + \beta^- p^- \tag{18}$$

$$\beta^\pm = \begin{cases} \frac{1}{4} (2 \mp M^\pm) (M^\pm \pm 1)^2, & |M^\pm| < 1 \\ \frac{1}{2} (1 + \text{sign}(\pm M^\pm)) & , \text{ otherwise} \end{cases} \tag{19}$$

This is rewritten exactly as<sup>[9]</sup>,

$$\tilde{p} = \frac{p^+ + p^-}{2} + \frac{\beta_+ - \beta_-}{2} (p^+ - p^-) + (\beta_+ + \beta_- - 1) \frac{p^+ + p^-}{2} \tag{20}$$

In low Mach number flow, by neglecting higher order term, the last term approaches to;

$$(\beta_+ + \beta_- - 1) \frac{p^+ + p^-}{2} \Rightarrow \frac{3}{4\gamma} \frac{\rho^+ + \rho^-}{2} \bar{c} (V_n^+ - V_n^-), \quad (21)$$

where slightly different definition of  $\bar{c}$  from other part of this paper shown below is used;

$$\bar{c} = \sqrt{\gamma \frac{p^+ + p^-}{\rho^+ + \rho^-}}, \quad (22)$$

Thus this term behaves as numerical viscosity. Scaling the numerical viscosity to the proper amount can be achieved by multiplying the non-dimensional coefficient that is proportional to Mach number in low Mach number regime. The coefficient must approach to unity at transonic speed to maintain stability. The simplest but effective form is written as,

$$\tilde{p} = \frac{p^+ + p^-}{2} + \frac{\beta^+ - \beta^-}{2} (p^+ - p^-) + \min(1, \max(M^+, M^-)) (\beta_+ + \beta_- - 1) \frac{p^+ + p^-}{2} \quad (23)$$

$$\hat{M} = \frac{\sqrt{u^2 + v^2 + w^2}}{c} \quad (24)$$

Combining the mass flux defined by Eq.(17) and the pressure term defined above, the new Riemann flux LSHUS (Low-dissipation SHUS) is formulated. Since the difference between LSHUS and SHUS is only the modification in Eq.(23), the increase of computational cost is negligible. Note that LSHUS behaves exactly the same as SHUS in supersonic flow. Therefore it keeps robustness when proper limiter is used in MUSCL. Although they are not shown in this paper, LSHUS gives identical results with Roe and SHUS for the standard shock tube problems. The benefits and the performance of LSHUS are shown by computational results in Section 3.

## 2.4 Relationship to preconditioning

The present study is similar to the preconditioning matrix method<sup>[1-3]</sup> in the sense that it makes possible to use the compressible flow CFD method for very low mach number flows. The preconditioning matrix works in two phase in preconditioned flow solvers. Firstly, the matrix works on the time integration. The preconditioned Navier-Stokes equation written in the finite volume form is;

$$\Gamma \frac{V_i}{\Delta t_i} \Delta \mathbf{Q}_i + \sum_j (\tilde{\mathbf{E}}_{i,j} - \tilde{\mathbf{R}}_{i,j}) s_{i,j} = 0, \quad (25)$$

where  $\Gamma$  is the preconditioning matrix. This affects only the time dependent behavior, thus the converged solution is independent of  $\Gamma$ . This modification makes compressible flow solvers converge significantly fast to the steady states for very low Mach number flows and is quite effective with LSHUS too. The convergence of the drag of the circular cylinder in inviscid flow at Mach 0.001 is shown in Fig.1 for comparison. As shown in the figure, LSHUS combined with the preconditioning gives the converged value in some hundreds steps, on the other hand, un-preconditioning one does not even after 10 thousands of steps.

Secondary, the numerical dissipation of the scheme should be scaled by the preconditioning matrix in order to ensure stable computation with the preconditioning on time integration. The example for Roe scheme is shown below. The numerical flux of original Roe scheme is written as;

$$\tilde{\mathbf{F}} = \frac{1}{2} \left\{ \tilde{\mathbf{E}}^+ + \tilde{\mathbf{E}}^- - |\mathbf{A}| (\mathbf{Q}^- - \mathbf{Q}^+) \right\} \quad (26)$$

where  $|\mathbf{A}|$  is the Jacobian matrix of inviscid flux whose eigenvalues are replaced by the absolute value of them. Preconditioned Roe scheme is defined by;

$$\tilde{\mathbf{F}} = \frac{1}{2} \left\{ \tilde{\mathbf{E}}^+ + \tilde{\mathbf{E}}^- - |\Gamma^{-1} \mathbf{A}| (\mathbf{Q}^- - \mathbf{Q}^+) \right\} \quad (27)$$

This modification of flux reduces numerical dissipation in low Mach number regime, thus affects the converged solution. LSHUS has low dissipation nature by itself, therefore it need not the help from  $\Gamma$  for dissipation control. LSHUS has no problem depending parameter that is indispensable in the numerical viscosity preconditioning. Moreover LSHUS is more robust than the preconditioning Roe scheme. Because LSHUS scheme approaches to SHUS in high Mach number, which is more robust than Roe scheme, while the latter approached to Roe scheme.

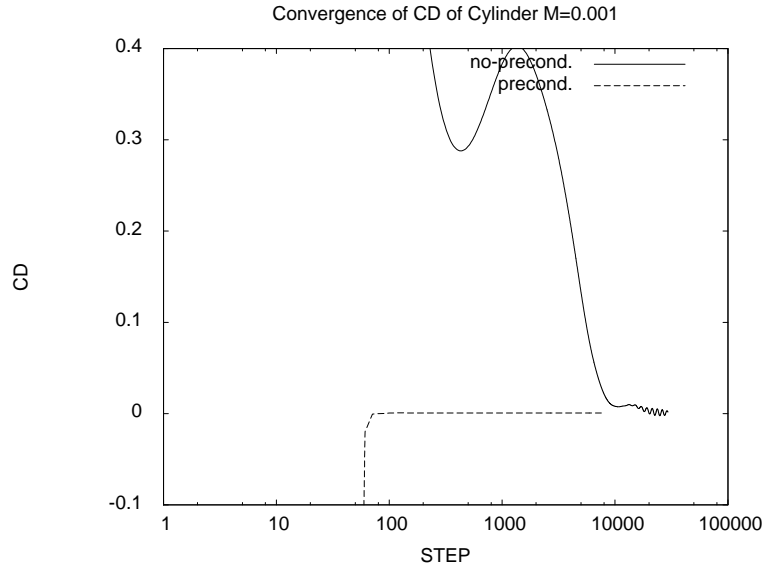


Figure 4. Convergence histories of computed drag coefficient of a cylinder in inviscid flow at  $M_\infty=0.001$ .

### 3 NUMERICAL RESULTS

A series of test results are presented in the following: Firstly, low dissipative nature of scheme is shown by the drag estimation of circular cylinder in various Mach number flows, then very low speed flow computations including vortices, sound propagation and aero-acoustic simulations are demonstrated, followed by hypersonic flow past a cylinder. The third-order MUSCL without limiter is employed along with implicit time integrations in these computations,<sup>[14]</sup> if not mentioned otherwise. The implicit time integration method is also shown in APPENDIX.

#### 3.1 D'Alembert's paradox

It is known as D'Alembert's paradox that the two dimensional object in inviscid subsonic flow has no aerodynamic drag. Therefore the drag calculated numerically gives an indication of an error of the scheme. The drag coefficients of a circular cylinder in inviscid flow at sev-

eral Mach numbers are shown in Fig.(2). Excessive numerical dissipation in Roe scheme and AUSM produce huge error at very low Mach number. On the other hand that of LSHUS gives much lower and almost constant value.

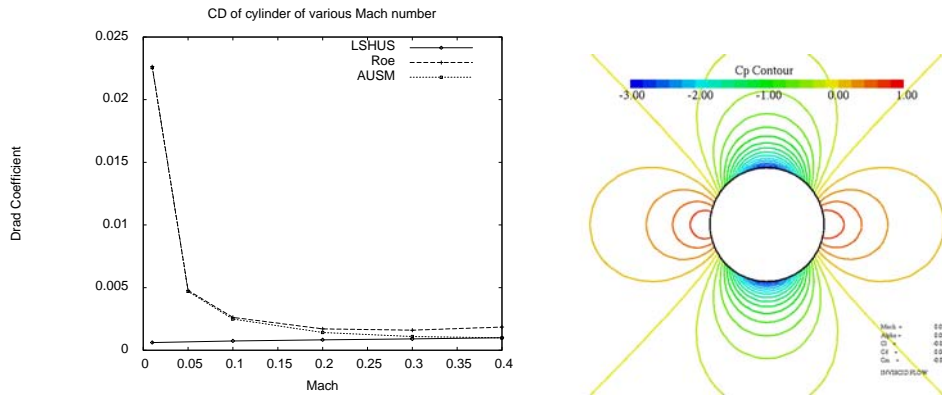


Figure 2: Drag of cylinder in inviscid flow. Cd vs. Mach(left) and Cp contour at Mach=0.01(right)

### 3.2 Rankine vortex

A static Rankine vortex, of which radius is twice as large as grid size and peak Mach number is 0.01, is computed by several methods. As shown in Fig.(3,4), results by Roe scheme and AUSM are smeared, on the other hand that of LSHUS almost keeps the initial shape.

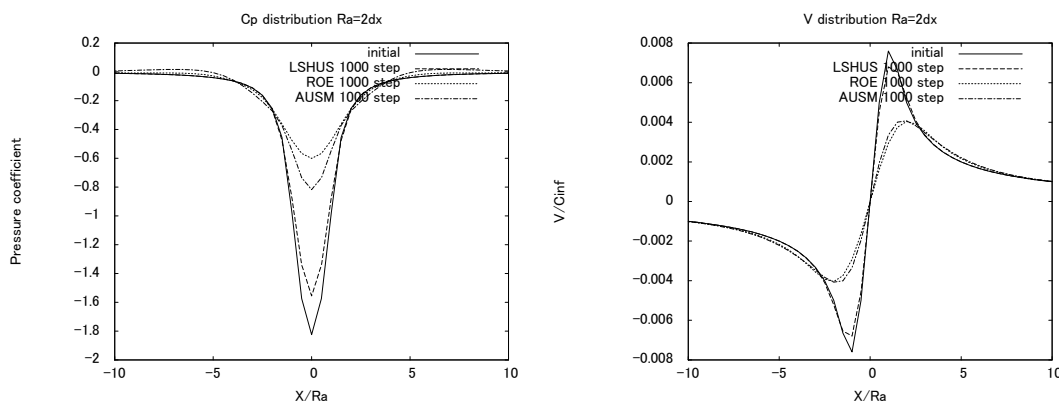


Figure 3: Cp(left) and velocity distribution(right) of a Rankine vortex after 1000 step.

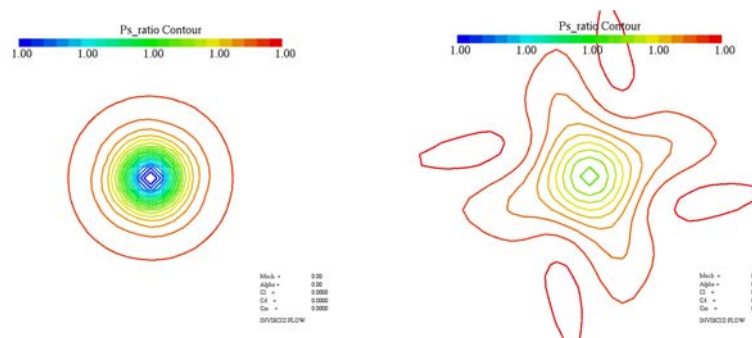


Figure 4: Pressure contour of a Rankine vortex after 1000 step. LSHUS(left) and Roe(right)



### 3.3 1D sound propagation

As the present scheme is based on the compressible flow equation, the sound propagation can be computed directly (Fig.(5)). LSHUS is less dissipative than Roe scheme.

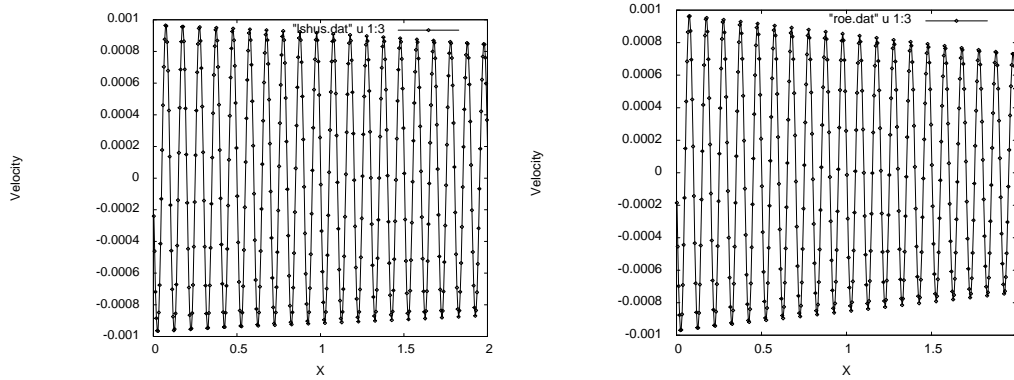


Figure 5: Velocity of one dimensional sound propagation. LSHUS(left) and Roe(right).

### 3.4 Sound wave generated by Karman vortices

As shown earlier, LSHUS has better accuracy in aerodynamics and sound propagation analysis, thus it is expected to have better accuracy in aero-acoustic problem. LSHUS captures fine vortices more sharply and higher frequency pressure fluctuation.(Fig.(6))

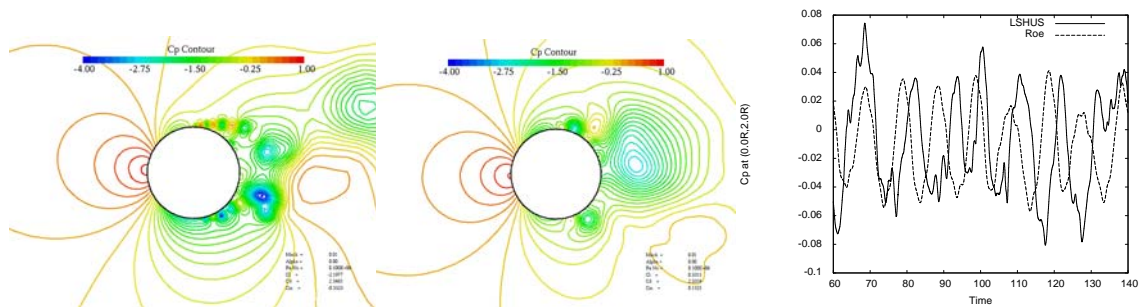


Figure 6: Cp contour by LSHUS(left), Roe(center) and Cp history of the side point at two radius distance from the center.  $M=0.01$ .

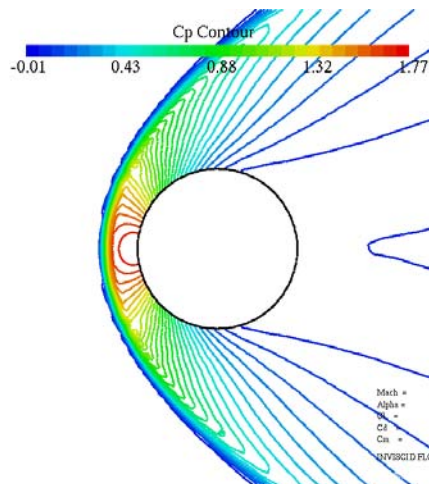


Figure 7: Cp contour of inviscid flow at Mach 10 past a cylinder

### 3.5 Inviscid hypersonic flow past a cylinder

AUSM family schemes are originally developed seeking the robust algorithm at high Mach number regime. SHUS and LSHUS inherit that nature. As shown in Fig.(7), the flow at Mach 10 past a cylinder can be computed easily. Chakravarthy-Osher type MUSCL reconstruction with slope limiter<sup>[15]</sup> is used in this computation. Note that the scheme is conservative, thus shock position and strength are correctly captured. Although the stable treatment for such shock and expansion is not necessary for low Mach number flow, the robustness ensures stability at low Mach number flows.

## 4 CONCLUSIONS

- Formulation of new Riemann flux function named LSHUS and results of test computations are shown.
- LSHUS is based on AUSM and inherits favorable natures, such as low dissipation for boundary layer, simplicity and robustness.
- Excessive numerical dissipation in low Mach number regime is reduced in the proper level by modifying the pressure term of AUSM family scheme.
- Although LSHUS does not employ the concept of the preconditioning matrix method, the combined use with the time integral preconditioning method is quite effective to accelerate convergence to the steady state in low Mach number regime.
- It is shown by numerical examples that the new scheme combined with proper time integration method can compute the flow from very low Mach to very high Mach number with keeping crisp capturing nature for vortex and shock.
- LSHUS can compute very low Mach number flow and sound propagation at the same time. Moreover LSHUS is less dissipative in the propagation of sound than the standard compressible method. Thus LSHUS is suitable for example, to computation of aero-acoustic sound generated by the bluff body.

## ACKNOWLEDGEMENTS

The author thanks to Dr.Shimizu of JAXA for reviewing this manuscript.

## APPENDIX: MFGS IMPLICIT SCHEME

As the difference of characteristic speeds becomes huge in low Mach number flows, numerical time step must be very small due to C.F.L condition, when the explicit time integration is used. Thus implicit time integration methods are low Mach number flows. A simple but effective implicit scheme is presented in this section.

The summation of the inviscid numerical flux with the viscous flux around the computational cell forms the right hand side (explicit residual) of implicit algorithm. The implicit algorithm is written as follows for a cell "i" in general finite volume formulation,

$$\begin{aligned}
 & \left( \frac{V_i}{\Delta t_i} + \sum_j s_{i,j} \tilde{\mathbf{A}}^+_{i,j} \right) \Delta \mathbf{Q}_i - \sum_j s_{i,j} \tilde{\mathbf{A}}^+_{j,i} \Delta \mathbf{Q}_j \\
 & = - \sum_j (\tilde{\mathbf{E}}_{i,j} - \tilde{\mathbf{R}}_{i,j}) s_{i,j}
 \end{aligned} \tag{A1}$$

where linearized first order upwind scheme is used to separate and simplify implicit term. Note that here  $\mathbf{A}_{i,j}^+$  denotes the part of the Jacobian matrix of flux function at cell interface between cell ‘‘i’’ and cell ‘‘j’’ that have only positive eigenvalues. The matrix is defined at cell i and the positive direction is from ‘‘i’’ to ‘‘j’’.

The L.H.S. forms a large sparse matrix and the matrix is solved approximately using symmetric Gauss-Seidel relaxation algorithm in this study. We adopt approximate flux Jacobians proposed in Yoon & Jameson’s LU-SGS<sup>[16]</sup> scheme;

$$\tilde{\mathbf{A}}^+_{i,j} \approx \frac{\tilde{\mathbf{A}}_{i,j} + \sigma_{i,j} I}{2}, \tag{A2}$$

where  $\sigma$  is a spectral radius of the Jacobian matrix and that is given as follows adding viscous flux contribution.

$$\sigma_{i,j} = |V_{ni,j}| + c_i + \frac{2(\mu + \mu_T) s_{i,j}}{\rho_i V_i}, \tag{A3}$$

By introducing these approximations, the Gauss-Seidel iteration for implicit scheme is greatly simplified as follows.

$$\begin{aligned}
 & \Delta \mathbf{Q}^{new}_i \\
 & = \left\{ \sum_j s_{i,j} \tilde{\mathbf{A}}^+_{j,i} \Delta \mathbf{Q}_j - \sum_j (\tilde{\mathbf{E}}_{i,j} - \tilde{\mathbf{R}}_{i,j}) s_{i,j} \right\} / \left( \frac{V_i}{\Delta t_i} + \sum_j s_{i,j} \frac{\sigma_{i,j}}{2} \right), \\
 & \because \sum_j s_{i,j} \tilde{\mathbf{A}}_{i,j} = 0
 \end{aligned} \tag{A4}$$

where the latest values in the iteration is used in R.H.S.

By using reverse linearization<sup>[17]</sup>, matrix operation in R.H.S. can be eliminated as follows.

$$\tilde{\mathbf{A}}^+_{j,i} \Delta \mathbf{Q}_j \approx \frac{\hat{\mathbf{E}}_{j,i}(\mathbf{Q}_j^n + \Delta \mathbf{Q}_j) - \hat{\mathbf{E}}_{j,i}(\mathbf{Q}_j^n) + \sigma_{j,i} \Delta \mathbf{Q}_j}{2}, \tag{A5}$$

$$\hat{\mathbf{E}}_{j,i} = \begin{pmatrix} \rho V_n \\ \rho u V_n + p x_n \\ \rho v V_n + p y_n \\ \rho w V_n + p z_n \\ (e + p) V_n \end{pmatrix}, \tag{A6}$$

where  $\hat{E}$  is merely the inviscid flux defined by the governing equation and is not an upwind numerical flux.

Implicit flux summation in R.H.S. can be further simplified by shifting the defining point of cell center value and using Gauss’s theorem;

$$\begin{aligned}
& \sum_j s_{i,j} \tilde{\mathbf{A}}_{j,i}^+ \Delta \mathbf{Q}_j & (A7) \\
& \approx \sum_j s_{i,j} \frac{\hat{\mathbf{E}}_{j,i}(\mathbf{Q}_j^n + \Delta \mathbf{Q}_j) - \hat{\mathbf{E}}_{j,i}(\mathbf{Q}_j^n) + \sigma_{j,i} \Delta \mathbf{Q}_j}{2} \\
& \approx \sum_j s_{i,j} \frac{\hat{\mathbf{E}}_{j,i}(\mathbf{Q}_i^n + \Delta \mathbf{Q}_j) - \hat{\mathbf{E}}_{j,i}(\mathbf{Q}_i^n) + \sigma_{i,j} \Delta \mathbf{Q}_j}{2}, \\
& = \sum_j s_{i,j} \frac{\hat{\mathbf{E}}_{j,i}(\mathbf{Q}_i^n + \Delta \mathbf{Q}_j) + \sigma_{i,j} \Delta \mathbf{Q}_j}{2} \\
& \because \sum_j s_{i,j} \hat{\mathbf{E}}_{j,i}(\mathbf{Q}_i^n) = -\sum_j s_{i,j} \hat{\mathbf{E}}_{i,j}(\mathbf{Q}_i^n) = 0
\end{aligned}$$

Final form of the iterative procedure is given by,

$$\begin{aligned}
& \Delta \mathbf{Q}_i^{new} & (A8) \\
& = \left\{ \sum_j s_{i,j} \frac{\hat{\mathbf{E}}_{j,i}(\mathbf{Q}_i^n + \Delta \mathbf{Q}_j) + \sigma_{i,j} \Delta \mathbf{Q}_j}{2} \right. \\
& \quad \left. - \sum_j (\tilde{\mathbf{E}}_{i,j} - \tilde{\mathbf{R}}_{i,j}) s_{i,j} \right\} / \left( \frac{V_i}{\Delta t_i} + \sum_j s_{i,j} \frac{\sigma_{i,j}}{2} \right)
\end{aligned}$$

Note that this scheme has no matrix operation and then its simplicity is comparable to Gauss-Seidel iteration for Poisson equation for pressure term which is used in MAC method for incompressible flow CFD method.

The scheme uses the same approximate Jacobian matrix, hence it is similar to LU-SGS<sup>[16]</sup>. However, it is not appropriate to name it as a variant of “LU-SGS”. Because, the essence of general “LU-SGS” is to simplify Gauss-Seidel iteration procedure by limiting number of sweep to only one reciprocal one. On the other hand, the present scheme is rather based on the original Gauss-Seidel sweep and can be used with arbitrary number of sweeps. Thus this scheme is named as MFGS (Matrix Free Gauss-Seidel method). Note that the Gauss-Seidel iteration in the implicit scheme for the compressible flow CFD method needs not to converge. It is why only one pair of reciprocal sweeps in LU-SGS is acceptable. The optimal number of sweeps, however, is not necessarily two. MFGS computations with several inner iteration counts are compared in Fig.A1. As shown in the figure, 10 to 20 pairs of reciprocal sweeps give best convergence rate to the CPU time. Note that the line titled “2 iterations” in the figure indicates approximate performance of LU-SGS. Thus the present method gives several times faster convergence than LU-SGS. Our separate research indicates that the same number of sweeps is appropriate for unsteady computation and combination with dual time stepping.

MFGS can be used both for structured grid method and unstructured grid method. Here the performance of MFGS for structured grid method is shown. The diagonalized ADI method is known to be simple and fast method for structured grid method. In Fig.A2, the convergence to the steady states of MFGS and the diagonalized ADI are compared. It is shown that MFGS is slightly faster than the diagonalized ADI.

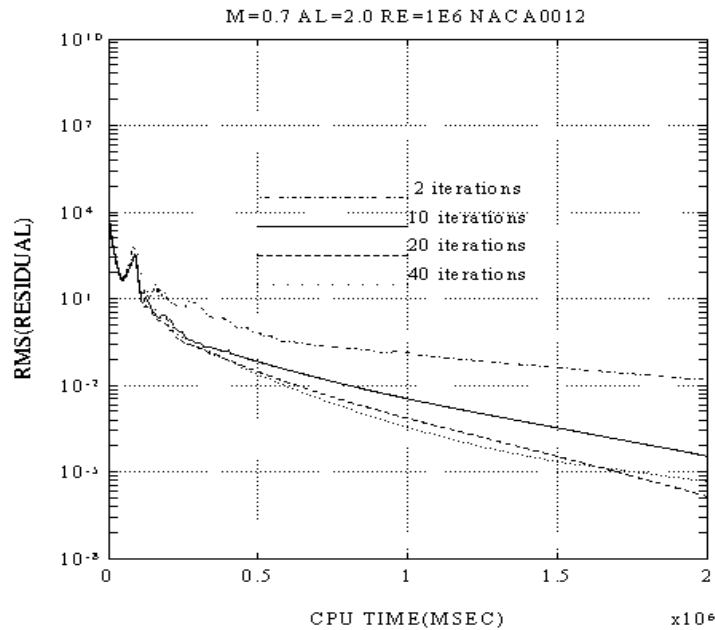


Figure A1 Convergence history of NS computation around NACA0012 Airfoils. Several Gauss-Seidel iteration counts are compared.

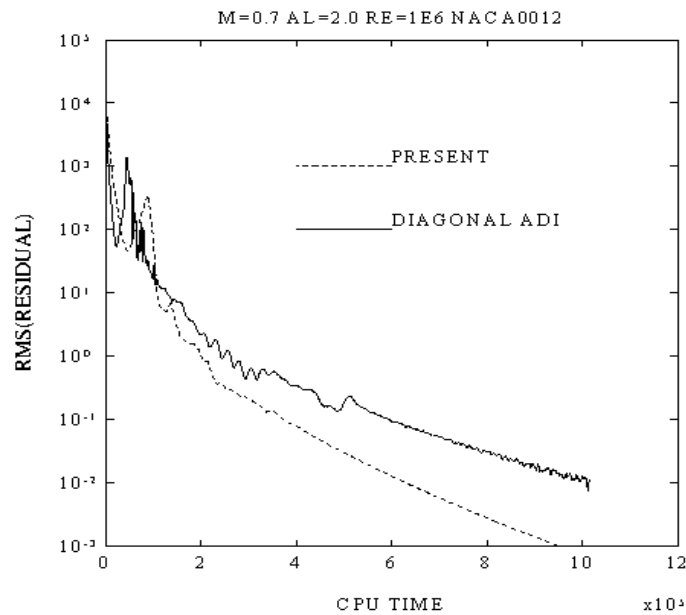


Figure A2 Convergence to steady states of MFGS and diagonalized ADI algorithm.

One of the benefits of this method is the capability of using quite large Courant number, because this does not have factorization error that is contained in ADI method. This feature is quite beneficial for compressible CFD method to solve very low Mach number flows.

The implicit time integration methods are less accurate for unsteady flow problems than the explicit schemes, however, the loss of accuracy is acceptable when courant number is very small. Note that Courant number outside the boundary layer in high Reynolds number flow is usually very small even in low Mach number flow, because the time step size to compute is very small due to the very small mesh size necessary to capture thin boundary layer. Thus implicit time integration is good enough even for sound in practical computations, except sound

propagation in boundary layers is required. Either the dual time stepping method or the second order time accurate method will improve the accuracy, although it is not demonstrated here.

## REFERENCES

- [1] E.Turkel, Preconditioning Technique in Computational Fluid Dynamics, *Annu. Rev. Fluid Mech*, **31**, 385-416, 1999
- [2] J.M.Weiss and W.A.Smith, Preconditioning Applied to Variable and Constant Density Flows, *AIAA Journal*, **33**, 2050–2057, 1995
- [3] D.Unra and D.W.Zingg, Viscous Airfoil Computations Using Local Preconditioning, *AIAA Paper 97-2027*, 1997.
- [4] P.L.Roe, Approximate Riemann Solvers, Parameter Vectors, and Difference Schemes, *Journal of Computational Physics*, **43**, 357–372, 1981
- [5] M.-S.Liou and C.J.Steffen Jr., A New Flux Splitting Scheme, *Journal of Computational Physics*, **107**, 23–39, 1993
- [6] Y.Wada and M.-S.Liou, A Flux Splitting Scheme with High-Resolution and Robustness for Discontinuities, *AIAA Paper 94-0083*, 1994.
- [7] M.-S.Liou, A Sequel to AUSM: AUSM+, *Journal of Computational Physics*, **129**, 364–382, 1996
- [8] E.Shima and T.Jounouchi, Role of CFD in Aeronautical Engineering (No.14) - AUSM Type Upwind Schemes-, *NAL-SP30, Proceedings of 13th NAL symposium on Aircraft Computational Aerodynamics*, 41-46, 1996
- [9] J.R.Edwards, Towards Unified CFD Simulation of Real Fluid Flows, *AIAA Paper 2001-2524*, 2001.
- [10] M.-S.,Liou, A Sequel to AUSM, Part II: AUSM+-up for all speeds, *Journal of Computational Physics*, **214**, 137-170, 2006
- [11] M.-S.Liou, Mass Flux Schemes and Connection to Shock Instability, *Journal of Computational Physics*, **160**, 623-648, 2000
- [12] X.-S. Li and C.-W. Gu, An All-Speed Roe-type scheme and its asymptotic analysis of low Mach number behaviour, *Journal of Computational Physics*, **227**, 5144 - 5159, 2008
- [13] B.Van Leer, Flux-Vector Splitting for the Euler Equations, *Lecture Notes in Physics*, **170**, 507–512, 1982
- [14] E.Shima, A Simple Implicit Scheme for Structured/Unstructured CFD, *Proceedings of 29th Fluid Dynamic Conference*, 325-328, 1997 (in Japanese)
- [15] S.R.Chakravarthy and S.Osher, A New Class of High Accuracy TVD Schemes for Hyperbolic Conservation Laws, *AIAA Paper 85-0363*, 1985
- [16] Yoon,S. and Jameson,A., “Lower-upper symmetric-Gauss-Seidel method for the Euler and Navier-Stokes equations”, *AIAA J.*, Vol.26, No.8, p 1025-1026, 1988

- [17] I. Menshov, Y. Nakamura, An Implicit advection upwind splitting scheme for hyperbolic air flows in thermochemical nonequilibrium, *6th International Symposium on CFD*, 1995